ATP-dependent structural change of the eukaryotic clamp-loader protein, replication factor C

Yasushi Shiomi*, Jiro Usukura†, Yusuke Masamura‡, Kunio Takeyasu‡, Yoshikazu Nakayama§, Chikashi Obuse*, Hiroshi Yoshikawa*, and Toshiki Tsurimoto*¶

*Nara Institute of Science and Technology, Takayama, Ikoma, Nara 630-0101, Japan; †Department of Anatomy, Nagoya University, School of Medicine, Nagoya 466-0065, Japan; ‡Laboratory of Plasma Membrane and Nuclear Signaling, Graduate School of Biostudies, Kyoto University, Kyoto 606-8591, Japan; and §Department of Physics and Electronics, Osaka Prefecture University, 1-1 Gakuen-Cho Sakai, Osaka 599-8531, Japan

Communicated by Bruce Alberts, National Academy of Sciences, Washington, DC, October 25, 2000 (received for review April 14, 2000)

The eukaryotic DNA sliding clamp that keeps DNA polymerase engaged at a replication fork, called proliferating cell nuclear antigen (PCNA), is loaded onto the 3′ ends of primer DNA through its interaction with a heteropentameric protein complex called replication factor C (RFC). The ATPase activity of RFC is necessary for formation of a functional PCNA clamp. In the present study, the sensitivity of RFC to partial proteolysis is used to show that addition of ATP, ATPγS, or ADP induces different structural changes in RFC. Direct observation by electron microscopy reveals that RFC has a closed two-finger structure called the U form in the absence of ATP. This is converted into a more open C form on addition of ATP. In contrast, the structural changes induced by ATPγS or ADP are limited. These results suggest that RFC adapts on opened configuration intermediately after ATP hydrolysis. We further observe that PCNA is held between the two fingers of RFC and propose that the RFC structure change we observe during ATP hydrolysis causes the attached PCNA to form its active ring-like clamp on DNA.

During DNA replication, a highly organized protein-DNA complex is formed at the replication fork, which proceeds along double-helical DNA synthesizing leading and lagging strands in coordination (1–4). The complex consists of more than 10 components, highly conserved across organisms in terms of structure and function (5–7). Intensive studies on the DNA polymerases at prokaryotic replication forks have revealed that they form dimers, synthesizing the two strands in different modes simultaneously (1, 8). Despite progress with prokaryotic systems, the precise configuration of proteins at a eukaryotic replication fork is still poorly understood, and at least three different DNA polymerases, α, δ, and ε, are thought to exhibit independent roles in the fork (9, 10). Best understood is the *in vitro* replication system for simian virus 40 virus DNA, in which the replication fork has been reconstituted with DNA polymerases α and δ and the accessory proteins, PCNA and RFC (11, 12). PCNA functions as a DNA sliding clamp, as also reported for the *Escherichia coli* DNA polymerase III β subunit and T4 phage gene 45 protein (13–15). Biochemical and crystallographic studies have shown that these clamps all have a characteristic ring structure, formed by a homomultimeric subunit complex that slides freely in both directions along the double-helical DNA, which is threaded through it (16–19).

DNA polymerases, which intrinsically have a limited affinity for DNA, are stabilized on a template DNA by their sliding clamps and thereby synthesize DNA processively (17, 20, 21). The loading and unloading of clamps would be expected to be controlled during DNA synthesis. For example, repeated loading and unloading will occur during lagging-strand synthesis, whereas unloading will be minimal during leading-strand synthesis. Although the detailed mechanisms regulating loading and unloading of these clamps have not been elucidated, loading requires a temporary opening of the closed ring to encircle the DNA (22). Because the head-to-tail connections of the monomer interfaces that form the ring are very stable due to hydrophobic interactions, opening is an energy-consuming step. Factors called clamp loaders are required, and RFC plays this role for PCNA in eukaryotes (23, 24). RFC is in a heteropentameric complex composed of one large (140 kDa) and four small subunits (40–36 kDa). It binds specifically to PCNA and the 3′ end of primer DNA, and it exhibits ATPase activity (25, 26). The five subunits of RFC individually have nucleotide-binding motifs and potential ATPase activity (23), and four of these subunits are essential for PCNA-loading activity (27). O'Donnell's group has studied the clamp-loading process in detail by using *E. coli* factors (28, 29) and confirmed that an opening of the β-subunit ring is driven by a structural change of its loader protein γ subunit caused by ATP binding. Thus, one would predict that RFC would also change its structure in an ATP-dependent manner and thereby drive the temporary opening of the PCNA ring.

Here, we show there is a dynamic alteration of the interaction between RFC and PCNA caused by ATP hydrolysis. Furthermore, we examine the structural change produced in RFC by ATP hydrolysis by using both biochemical methods and electron microscopy (EM). Our data strongly suggest that the structural change of RFC caused by ATP hydrolysis promotes an opening of the attached PCNA and its loading onto DNA.

Materials and Methods

Purification of Proteins. Human PCNA was purified from *E. coli* harboring pT7-PCNA by using three column chromatography steps, as published earlier (30). Human RFC was prepared from insect cells (SF9) infected with a mixture of baculoviruses carrying all the human RFC genes by affinity chromatography on a PCNA–agarose column by a procedure modified from a previous method (24).

Surface Plasmon Resonance Analyses. All procedures were performed with BIACORE 2000 (Biacore, Uppsala, Sweden) in Running Buffer (10 mM Hepes–NaOH, pH 7.4/0.2 mM EDTA/10 mM $MgCl_2$/0.05% Tween 20/150 mM NaCl). PCNA (1×10^3 resonance units) was fixed on a sensor chip CM5 (Biacore), and kinetic experiments were performed after injection of various concentrations of RFC with or without 1 mM ATP, ATPγS, or ADP. Dissociation and association rate constants (k_{off} and k_{on}) were obtained for a simple binding model of A + B = AB by using BIAEVALUATION 3.0 software (Biacore), and K_D values were calculated as their ratios.

Abbreviations: PCNA, proliferating cell nuclear antigen; RFC, replication factor C; Lys-C, endopeptidase Lys-C; EM, electron microscopy; TEM, transmission EM; AFM, atomic force microscopy.

¶To whom reprint requests should be addressed. E-mail: turimoto@bs.aist-nara.ac.jp.

The publication costs of this article were defrayed in part by page charge payment. This article must therefore be hereby marked "*advertisement*" in accordance with 18 U.S.C. §1734 solely to indicate this fact.

BIOCHEMISTRY

Gel Mobility-Shift Assay of RFC. RFC (10 ng) was incubated in 10 μl of 10 mM Hepes–NaOH (pH 7.5)/10 mM $MgCl_2$/130 mM NaCl with or without 1 mM ATP at room temperature for 5 min, fixed with 0.1% glutaraldehyde at room temperature for 3 min, separated in a 4% acrylamide gel in Tris–glycine buffer (25 mM Tris/192 mM glycine, pH 8.3), and stained with silver (Dai-ichi Pure Chemicals, Tokyo). In the case of the PFC-PCNA complex, 6 ng of PCNA and 15 ng of RFC were incubated in 3 μl of 10 mM Hepes (pH 7.5)/0.2 mM EDTA/10 mM $MgCl_2$/0.05% Tween 20/150 mM NaCl with or without 1 mM ATP, ATPγS, or ADP at room temperature for 3 min and fixed and analyzed as above, except that the separation was performed on a 3–8% acrylamide gel (Tris-acetate, NuPAGE in Tris-glycine buffer; NOVEX, San Diego).

Partial Proteolysis. RFC (300 ng) was preincubated with 1 mM ATP, ATPγS, or ADP in 10 mM Hepes–NaOH (pH 7.5)/130 mM NaCl/10 mM $MgCl_2$, followed by digestion with 15 ng of endoprotease Lys-C (Lys-C; Promega) or 15 ng of trypsin (Sigma) at room temperature for 60 min. The digested peptides were separated in 4–12% gradient polyacrylamide gels (Bis-Tris SDS NuPAGE in NuPAGE Mes SDS running buffer; NOVEX) and stained with silver as above.

Transmission EM (TEM). Protein samples were incubated with or without 1 mM ATP at room temperature for 5 min in 20–30 μl of the buffer used for the partial proteolysis and fixed with 0.1% glutaraldehyde at room temperature for 3 min. Samples were mixed with Tris-HCl (pH 7.9) at final 100 mM and dialyzed on mixed cellulose ester membranes (type VM; Millipore) with 10 mM Hepes–NaOH (7.5)/0.01% Nonidet P-40/50 mM NaCl for 1 hour at 4°C. Glycerol was added to a final concentration of 50%, and the mixtures were sprayed onto freshly cleaved mica surfaces by using a painter's airbrush. The protein–glycerol drops on mica were dried in a vacuum (1×10^{-6} Pa) for 10 min at room temperature in a freeze-etching device (FR-7000, Hitachi, Tokyo) and cooled down to -100°C with liquid nitrogen. Subsequently, specimens were rotary shadowed with platinum at an angle of 2.5° to the mica surface, followed by carbon evaporation at an angle of 90°. The shadowed platinum films were removed from the mica by soaking into water and mounted on copper grids. Images were taken with a HitachiH-7100 electron microscope (access 100 k voltage) onto films at a magnification of $\times$100,000 and captured by using a Polascan 45 film scanner (Polaroid) (31–33). Images were further processed with Adobe PHOTOSHOP software (Adobe Systems, Mountain View, CA).

Atomic Force Microscopy (AFM). RFC was fixed in the presence or absence of ATP as described above, mounted on a freshly cleaved mica surface, incubated for 0.5–3 min, washed gently with water, and dried under nitrogen gas. AFM imaging in air by tapping was carried out at room temperature in the height mode with a scanning rate of 3–4 Hz by using a Nanoscope IIIa with a type E scanner (Digital Instruments, Santa Barbara, CA) (34). As scanning probes, we used conventional probes made of a single-silicon crystal with a cantilever length of 129 nm and a spring constant of 33–62 Newton/meter (Digital Instruments) or those attached with a carbon nanotube (ref. 35; ϕ = 5 nm). Images were captured in a 512 $\times$ 512 pixel format, flattened, plain fitted, and analyzed with NANOSCOPE software (Digital Instruments).

Results

Alteration of the Interaction Between RFC and PCNA. The relation between ATP hydrolysis by RFC and the strength of the RFC–PCNA interaction is of interest, because ATP is required for the PCNA-loading process (36, 37). Their affinity of binding

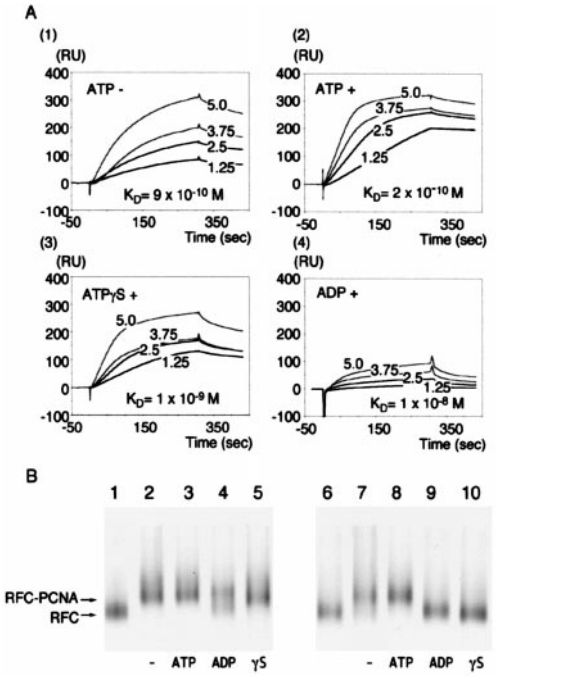

Fig. 1. Studies of the interaction between RFC and PCNA. (*A*) Surface plasmon resonance analyses. Indicated concentrations of RFC were injected into a sensor chip prefixed with about 1,000 resonance units of PCNA. All of the procedures were performed with 150 mM NaCl Running Buffer, with RFC as the analyte without nucleotides (1) or with 1 mM ATP (2), ATPγS (3), or ADP (4). K_D values with SD obtained from three injections were $(1 \pm 0.4) \times 10^{-9}$ M $(2 \pm 0.5) \times 10^{-10}$ M $(9 \pm 2) \times 10^{-10}$ M and $(1 \pm 0.8) \times 10^{-8}$ M, respectively. (*B*) Gel mobility profiles of RFC and RFC-PCNA complexes without ATP (–, lanes 2 and 7), with ATP (lanes 3 and 8), with ADP (lanes 4 and 9), or with ATPγS (lanes 5 and 10) at 0.15 M (lanes 1–5) or 0.5 M (lanes 6–10) NaCl. Arrows indicate migration positions of silver-stained RFC and RFC-PCNA complex. In lanes 1 and 6, only RFC was applied. PCNA runs at the dye front and does not appear in this picture under these electrophoresis conditions.

to each other in the absence or presence of ATP, ATPγS, or ADP was compared by the surface plasmon resonance method (38). The results are shown in Fig. 1*A*. In the absence of ATP, RFC has a significant affinity for PCNA, with a dissociation constant, K_D, of 9×10^{-10} M. In the presence of excess ATP, the K_D decreases to 2×10^{-10} M, representing binding that is about five times stronger than without ATP. To determine whether this increase occurs with ATP binding alone, we measured the affinity in the presence of ATPγS, a poorly hydrolyzed analogue of ATP. The K_D observed was 1×10^{-9} M, an even weaker binding than that found without ATP. The ADP-bound form of RFC is an even worse binder, with a $K_D = 1 \times 10^{-8}$ M, two orders of magnitude weaker than with ATP. It should be noted that ATPγS is a good ATP mimic for RFC, because the K_i value of ATPγS for RFC ATPase was calculated to be lower than the K_m value for ATP according to analysis with budding yeast RFC (39). Furthermore, ATPγS and ADP at 1 mM would be saturated for these experiments, because their addition at 0.1 mM made almost the same binding profiles. Thus, the interaction between RFC and PCNA would seem to be strongest for a transient conformation that follows ATP hydrolysis.

The above results are supported by native-gel electrophoresis of PCNA-RFC complexes crosslinked with glutaraldehyde under different conditions. PCNA-bound RFC was distinguishable from free RFC by a decrease in its mobility (Fig. 1*B*). Under physiological salt conditions (0.15 M NaCl), the complex is observed under all conditions, except with ADP as the nucleotide. When we increased the NaCl concentration to 0.5 M, the

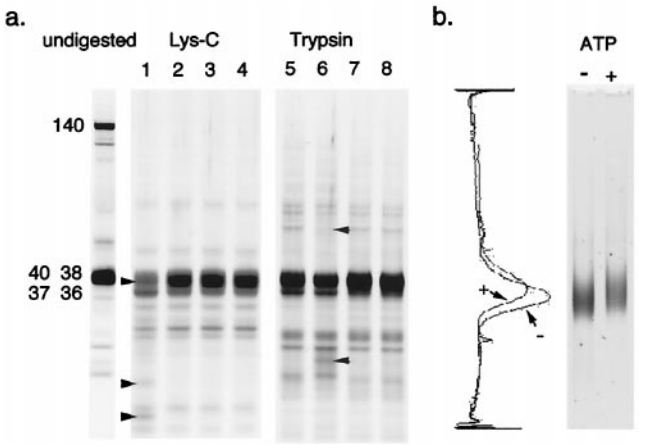

Fig. 2. Changes in RFC conformation under various conditions, as determined by its partial proteolysis profile (*a*) and migration in native-gel electrophoresis (*b*). (*a*) RFC was incubated with Lys-C (*Left*) or trypsin (*Right*) in the absence of nucleotides (lanes 1 and 5 or in the presence of ATP (lanes 2 and 6), ATPγS (lanes 3 and 7) or ADP (lanes 4 and 8), after which the digestion profiles were assessed by electrophoresis in SDS-polyacrylamide gels. Arrowheads are for bands whose appearance was changed by the addition or omission of nucleotides. Molecular weights of RFC subunits are indicated. The small subunits are not separated under these conditions. (*b*) RFC was fixed with glutaraldehyde with (+) or without (−) ATP and analyzed by electrophoresis on a native polyacrylamide gel. Densitometric profiles of their bands are provided (*Left*).

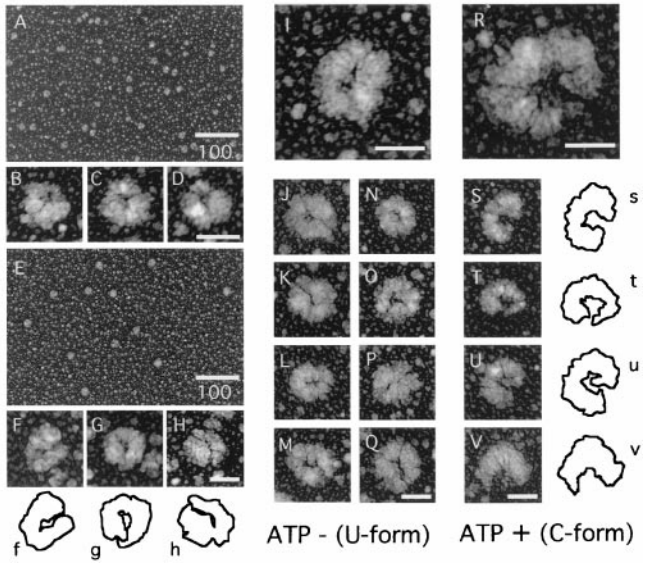

Fig. 3. Low-magnification images of PCNA (*A*) and RFC without ATP (*E*). *B–D* and *F–H* are high-power views from *A* and *E*. Standard length bars for *A* and *E* are 100 nm and for the others, 20 nm. The outlines of images for RFC in *F–H* are drawn below with *f–h*. Typical images of U- and C-form RFC obtained without and with ATP are shown in *I* and *R*, respectively. Examples of images of RFC in the U form without ATP (*J–Q*) and the C form with ATP (*S–V*) are shown. Outlines of images for the C form are drawn (*Right*) with *s–v*. The samples for *I–V* and *A–H* were prepared with and without crosslinking, respectively.

complex dissociated completely in the presence of ADP and ATPγS, partially in the absence of nucleotides but not at all in the presence of ATP. Thus the stability order of the RFC-PCNA complex is ATP > no nucleotide > ATPγS > ADP, consistent with the affinity constants measured by surface plasmon resonance above.

Alteration of the Proteolytic Digestion and Native Gel Electrophoresis Profiles in RFC. To obtain evidence of a structural change in RFC caused by ATP and its hydrolysis, we studied its partial Lys-C or trypsin digestion profiles in the presence or absence of ATP, ATPγS, or ADP. As indicated in Fig. 2*A*, the largest subunit was very sensitive to digestion with both proteases. With Lys-C digestion, intensities of the bands for the small subunits of 40–36 kDa were decreased specifically under ATP minus conditions, and two additional short peptides of 17 and 10 kDa appeared (arrowheads in lane 1). With trypsin digestion, addition of ATP resulted in a different profile from other conditions, and a band of 50 kDa disappeared and that of 21 kDa appeared specifically (arrowheads in lane 6). The results indicate that the structure of RFC differs in the presence or absence of ATP, and this structure is also distinguishable from those found in the presence of ATPγS or ADP.

The structures in the presence (+) or absence (−) of ATP were also studied by mobility shift on native gel electrophoresis after fixation with glutaraldehyde. A small but significant mobility shift of RFC could be detected (Fig. 2*B*, − and +). The migration in the presence of ATP, as shown by densitometric tracing, indicates that RFC becomes slightly more enlarged in shape and more heterogeneous in conformation. Addition of ATPγS or ADP resulted in no significant shift from the nucleotide minus condition (data not shown), indicating minimal effects on the conformation of RFC, if any.

TEM Observation of RFC Structure. We studied the structure of the individual RFC molecule by TEM after low-angle shadowing (31–33). With this method, PCNA appears as a ring composed of three units of similar size, as revealed previously by crystallography (Fig. 3 *A–D*). The average diameter from 190 observations was 18 ± 1.8 nm, indicating about 2-fold enlargement by shadowing. Examination of RFC in the absence of ATP before and after glutaraldehyde fixation (Fig. 3 *E–H* and *I–Q*) did not reveal any significant effect of fixation. In both cases, an oval structure with a cleft starting from one end of the longer axis was apparent, referred to as the "U form" on the basis of its shape. The average dimensions from 183 images of fixed samples were 33 ± 3.2 nm and 28 ± 2.9 nm for longer and shorter axes, respectively. If one assumes a constant enlargement factor of 2, we obtain the approximate size of RFC of 16 × 14 nm, in good agreement with a 290-kDa protein. We were able to distinguish five subunits aligned in a circle in some fine images (I, J, O, and Q).

Observation of an ATP-Dependent Structural Change in RFC by TEM. Most RFC molecules fixed in the presence of ATP appeared in U form, as also observed in the absence of ATP (data not shown). A significant population, however, exhibited what appears to be a different shape, referred to as the "C form," in which the cleft seemed to be opened to the sides (Fig. 3 *R–V*). Sixteen of 192 images, corresponding to 8% of the entire population, were judged to be obviously in this C form. In contrast, we were not able to detect this shape in 127 ATP-minus images. We believe that the population with this new shape is significant and that only a limited number of molecules show the structure, because we are fixing a heterogeneous population of molecules that are produced by ATP hydrolysis. The wider mobility distribution observed for the native gel electrophoresis in the presence of ATP (Fig. 2*B*) supports this interpretation.

The 8% C form could be an underestimation, as nearly one-half of the images seemed likely but not unequivocally to be in the C form in the population with ATP. This population could be intermediate between U and C forms in shape or might reflect the C form in a suboptimal orientation for observation. How-

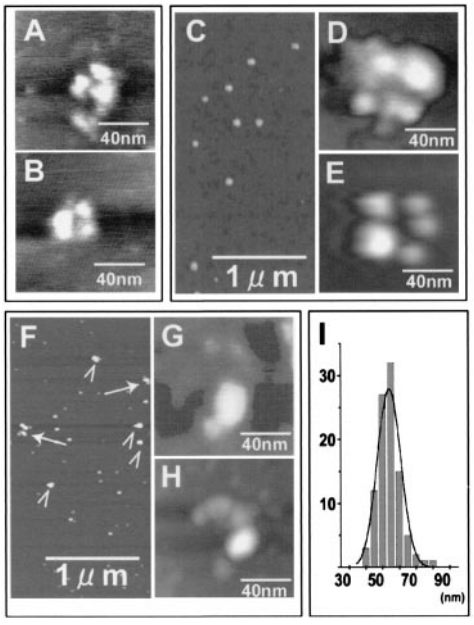

Fig. 4. AFM analyses of the subunit assembly and conformational change of RFC. AFM images of PCNA consisting of three homologous subunits (*A, B*), and RFC in the absence (*C, D*) or presence of ATP (*E–H*) at different magnifications. Images were obtained with regular cantilevers for *C, D, F,* and *G*, and with carbon nanotube tips for the rest, which provides a better lateral resolution. In *F*, arrows and arrowheads indicate open and closed forms of RFC, respectively. The frequency of finding the open forms was about 10% in more than 10 independent experiments. (*I*) A histogram that depicts the relationship between the frequency (ordinate) and the apparent size of closed forms without ATP measured through the cross section of the entire subunit complex (abscissa). A statistical analysis revealed that the average of the measured dimensions of the closed complex is 59.0 ± 7.0 nm ($n = 98$), which is reasonable considering the size of the conventional AFM tip. In the case of C form, the length of their longest cross section is 85.1 ± 1.9 nm ($n = 5$).

ever, only images that could be judged to be obviously in the C form were counted. We were unable to distinguish any obvious C-form RFC structures in the presence or absence of ATPγS or ADP (data not shown), suggesting that any structural changes in these conditions are subtle.

Demonstration of RFC Opening by AFM. To further examine RFC structural changes, we applied AFM, which allows analysis of native molecular structures directly (34). However, because of its limited resolution, AFM is not generally used for protein-structure studies. We applied both regular cantilevers of high quality or those harboring a nanocarbon fiber to obtain the high resolution (35). With the latter technique, we were able to distinguish the trimer configuration of PCNA (Fig. 4 *A* and *B*). When RFC structure was studied in the absence of ATP, images of a circular structure were observed (Fig. 4 *C* and *D*). In high magnifications, they consist of 5 particles aligned in a circle 59.0 ± 7.0 nm in diameter, probably corresponding to the U form by the TEM studies (Fig. 4*I*). In the presence of ATP, the major population appeared as a circular structure as above (Fig. 4 *E* and *F*), but about 10% of molecules demonstrated an open structure, with the subunits aligned in an arc 85.1 ± 1.9 nm at its longest cross section (Fig. 4 *F–H*), corresponding to the C form in Fig. 3.

Therefore, structure studies for RFC on the basis of two different principles have revealed exactly the same results in which a significant population of RFC appeared in the C form in the presence of ATP. Interestingly, we were able to distinguish five separate units by AFM, presumably corresponding to the five subunits. The second unit from one end of arc had a remarkably larger mass than the other units, suggesting that it corresponds to the largest subunit of RFC.

Two Fingers of RFC Hold PCNA. Taking the above observations into consideration, it is clear that RFC changes its structure during the hydrolysis of ATP. The next question is how the two-finger motion might fit with the PCNA-loading mechanism. To address this question, we studied the structure of RFC-PCNA complexes in the presence of ATP by TEM. As shown in Fig. 5 *A–C*, we detected images larger than both free RFC and PCNA in sizes and corresponding to RFC-PCNA complexes. From a strict viewpoint, it is difficult to distinguish where PCNA begins and RFC ends. As shown in *b* and *c*, however, we were able to interpret these images as separating into two parts reasonably, as indicated by their outlines. One part is the same as free PCNA in its shape and size. The other seems to correspond to RFC, because it can be superimposed with that of RFC alone in Fig. 3*R* and has five separable units characteristic for RFC. These results suggest that the two fingers of RFC hold PCNA between them. Because of limitations of image resolution, however, we could not detect a possible opening of the PCNA ring under this condition. Interestingly, most RFC-PCNA complexes were in the C form in the presence of ATP, although the observed number was not enough for statistics. In the absence of ATP, none of the complexes appeared in the C form, but images likely to be complexes between the U-form RFC and PCNA were observed (Fig. 5 *D–F*), as indicated by the difference of their dimensions (see Fig. 5 legend). In these images, one part could be superimposed with the U form of RFC and the other part with PCNA associated with the ends of RFC fingers (*e* and *f*). To confirm configuration of the PCNA-RFC complex precisely, further improvements to distinguish each component in TEM images will be necessary.

Discussion

The Conformation of RFC Induced by ATP. We have demonstrated that the interaction between RFC and PCNA is affected in the presence of ATP, ATPγS, or ADP, with the strongest affinity found in the presence of ATP. Because the ATPγS- and ADP-bound forms correspond to the ATP-bound and ATP-hydrolyzed situations, respectively, the high-affinity state induced by ATP may represent a transient intermediate. Proteolysis and native-gel electrophoresis experiments revealed that a structure in the presence of ATP could be distinguished from that not only without ATP but also with ATPγS or ADP. The structure with the latter two nucleotides was altered in a different fashion from that without ATP, as revealed by Lys-C digestion, although no remarkable differences were apparent in TEM images or by electrophoresis mobility. Therefore, multiple conformational states dependent on nucleotide were observed both by an affinity change between RFC and PCNA and by a structural analysis of RFC. The above data, combined with our EM results, suggest that the C form of RFC binds to PCNA most tightly.

When RFC ATPase activity is measured under the same conditions as for structural change, the hydrolysis rate is relatively slow in the absence of DNA, with two to three ATP hydrolyzed per minute per RFC molecule (data not shown). This hydrolysis rate becomes more than two times slower in the presence of PCNA (data not shown), suggesting that the structure change may stall in the C-form RFC-PCNA complex in the absence of DNA. Binding to DNA should release RFC from such stalling, because PCNA and DNA synergistically stimulate RFC ATPase activity (25). Thus, we propose that RFC-PCNA complexes form without DNA and find a target site by stalling in an intermediate state of ATP hydrolysis competent for DNA loading.

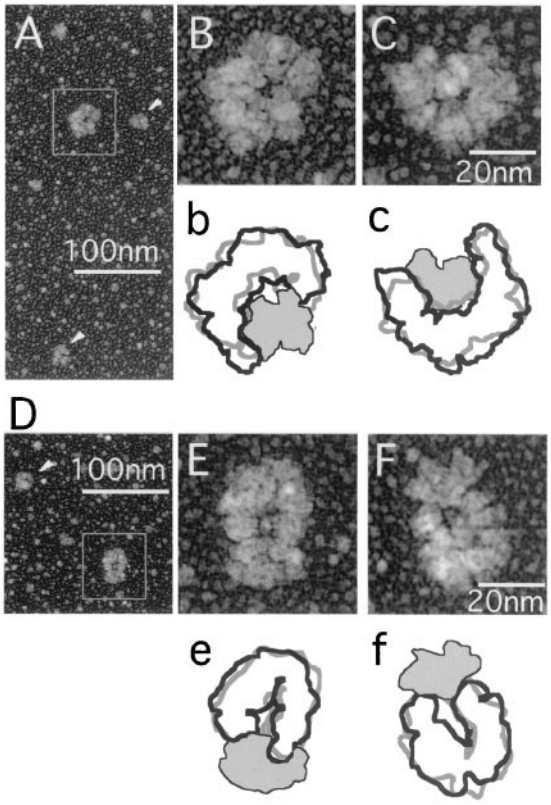

Fig. 5. TEM images of RFC-PCNA complexes. Low-power views of RFC-PCNA mixed sample in the presence (*A*) and absence of ATP (*D*). Arrowheads and boxes show images of free PCNA and RFC-PCNA complex, respectively. The standard bar length is 100 nm. Enlarged images of RFC-PCNA complexes in the presence and absence of ATP are shown in (*B*, *C*) and (*E*, *F*), respectively, with standard bars of 20 nm. The dimensions of the complexes are 37.1 ± 2.9 nm and 28.9 ± 4.9 nm at the longest and shortest axes in the presence of ATP (n = 10), and 44.2 ± 3.7 nm and 28.9 ± 3.6 nm in the absence of ATP (n = 10), respectively. The apparent difference in their ratios of axes,1.28 and 1.53, indicates the structural difference of the complex in the presence and absence of ATP. Interpreted outlines for RFC (thick lines) and PCNA (thin lines filled with shadow) are indicated below the images as *b*, *c*, *e*, and *f*. The overlapped gray lines are the outline of Fig. 3*R* for *b* and *c*, 3*F* for *e*, and 3*H* for *f*, respectively.

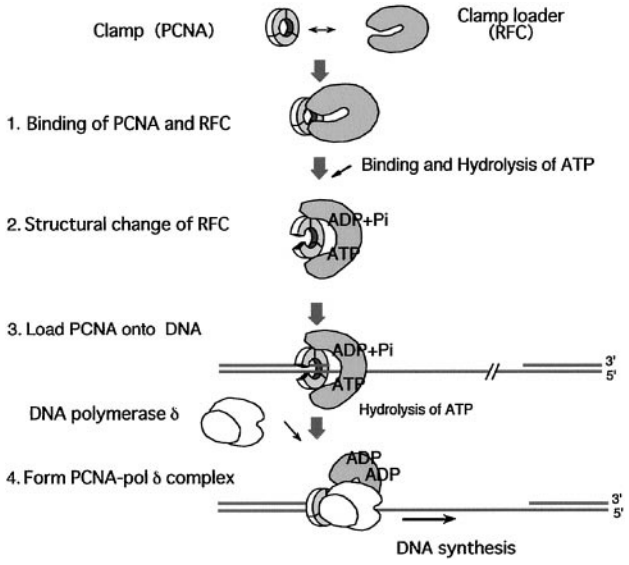

Fig. 6. A model for PCNA loading driven by RFC structural change. RFC associates with PCNA independent of ATP and changes its structure on binding and hydrolysis of ATP. Because both the prominent change in the structure of RFC and the loading of a functional PCNA clamp occur concomitantly by hydrolysis of ATP, the PCNA ring may open during the structural change. Some change in the PCNA structure may occur by binding of ATP, but the intermediate state formed during ATP hydrolysis produces the most pronounced structural change, to the C form, in which two fingers of RFC can hold PCNA strongly. This conformational change is proposed to open the PCNA ring to form a functional PCNA clamp on DNA. The C-form state of RFC corresponds either to an intermediate with bound ADP + P_i or to one with ATP hydrolysis of only some of the multiple bound ATPs. If the latter is the case, individual subunits might change their structure by stepwise hydrolysis of ATP, and the accumulation of this change would gradually open the whole RFC molecule to the C form. Through the structural change, the affinity between RFC and PCNA is decreased, and a functional PCNA clamp is formed on DNA, to which DNA polymerase δ is recruited. The number of ATPs that appear in this figure is arbitrary.

There are two possible explanations for the intermediate state observed in the presence of ATP. The first is that an ADP + P_i-bound state exists before P_i release to create the ADP-bound form, as reported for the intermediates of some ATPase reactions (40, 41). The second is that multiple ATP hydrolyses occur in a stepwise fashion during the process. The five subunits of RFC each have nucleotide-binding motifs and potential ATPase activity (23), and four of them are essential for PCNA-loading activity (27). If ATP hydrolysis by the four subunits occurs in a stepwise manner, the C form may be induced as an intermediate stage (Fig. 6). Such a stepwise ATP hydrolysis during the loading of the *E. coli* clamp β-subunit has been reported (42). Of course, a combination of these two types of explanations is also possible.

Structural Change and Loading. The present study demonstrates that the five subunits of RFC are aligned in a circle and suggests they work as two fingers, which can be opened through ATP hydrolysis. AFM images suggest the second subunit from one end is the 140-kDa subunit, the largest of the subunits. It is likely that this subunit has a special role in inducing opening of RFC and/or in binding to DNA. But elucidation of the precise order of subunits in the complex and their individual roles awaits future studies.

Our EM studies suggest that the two fingers of RFC hold PCNA. A likely process for loading PCNA by means of structural changes of RFC is diagrammed in Fig. 6. The PCNA-RFC complex is formed at the 3′ end of primer DNA in the presence of ATPγS (43, 44). Thus, some change in the PCNA structure may occur on binding of ATP to RFC, although no remarkable change in RFC structure was detected by TEM in the presence of ATPγS. On the other hand, the functional PCNA clamp is formed only in the presence of ATP (45–47), where we observe the C form of RFC. This C form may be important for transfer of the DNA bound PCNA to its functional state. Alternatively, one can claim that the structural change is independent of PCNA opening and functions mainly in the binding of RFC to DNA. This seems unlikely, because RFC has significant DNA-binding activity without ATP, and addition of ATPγS fully activates DNA binding when no prominent structure change of RFC has occurred.

Previous work has demonstrated that the Asp-41 and C-terminal tail of PCNA provide the site for interaction with RFC (30, 48). These sites are present in three places in the trimer ring. The EM images in the presence of ATP suggest that RFC fingers wrap around the PCNA ring, with multiple contacts between the two molecules. This situation presumably represents the most stable interaction in the presence of ATP. These contacts may change after completion of RFC ATP hydrolysis, facilitating recruitment of second partners—for example, DNA polymerase δ.

In conclusion, our studies have provided direct evidence that the clamp loader protein for PCNA changes its structure during ATP hydrolysis. This presumably drives opening of PCNA. We also showed that the affinity of RFC for PCNA changes drastically coupled with the structural change. The proposed mechanism could explain how functional protein complexes are formed during DNA replication, transcription, and recombination in an ATP hydrolysis-dependent manner. A significant number of proteins harbor multiple ATP-binding motifs in these reactions, and the importance of the ATP hydrolysis for their function has been demonstrated (49, 50). The protein structural change coupled with stepwise hydrolysis of ATP that we propose here might therefore be a general mechanism for loading or recruiting protein factors to target sites, with formation of functional complexes and transfer of reactions to second stages, as reviewed in ref. 51. Further biochemical and structural biological studies of the PCNA clamp-loading reaction should provide valuable insight into such reaction processes.

We thank Drs. H. Masukata of Osaka University and K. Mizuuchi of National Institutes of Health for their critical readings of this manuscript and valuable comments and Dr. M. Iwano of Nara Institute of Science and Technology and K. Hohmura of Kyoto University for their technical assistance during EM and AFM studies. This work was supported by grants in aid from the Ministry of Education, Science, Sports, and Culture of Japan.

1. Kelman, Z. & O'Donnell, M., (1995) *Annu. Rev. Biochem.* **64,** 171–200.
2. Nossal, N. G. (1992) *FASEB J.* **6,** 871–878.
3. Bambara, R. A., Murante, R. S. & Henricksen, L. A. (1997) *J. Biol. Chem.* **272,** 4647–4650.
4. Waga, S. & Stillman, B. (1998) *Annu. Rev. Biochem.* **67,** 721–751.
5. Baker, T. A. & Kornberg, A. (1992) in *DNA Replication* (Freeman, New York), 2nd Ed., pp. 478–483.
6. Stillman, B. (1989) *Annu. Rev. Cell. Biol.* **5,** 197–245.
7. Marians, K. J. (1992) *Annu. Rev. Biochem.* **61,** 673–719.
8. Lee, J., Chastain, P. D., II, Kusakabe, T., Griffith, J. D. & Richardson, C. C. (1998) *Mol. Cell* **7,** 1001–1010.
9. Burgers, P. M. J. (1995) *Methods Enzymol.* **262,** 49–62.
10. Sugino, A. (1995) *Trends. Biochem. Sci.* **8,** 319–323.
11. Tsurimoto, T., Melendy, T. & Stillman, B. (1990) *Nature (London)* **346,** 534–539.
12. Waga, S. & Stillman, B. (1994) *Nature (London)* **369,** 207–212.
13. Hubscher, U., Maga, G. & Podust, V. N. (1996) in *DNA Replication in Eukaryotic Cells*, ed. De Pamphilis, M. L. (Cold Spring Harbor Lab. Press, Plainview, NY), pp. 525–543.
14. Jonsson, Z. O. & Hubscher, U. (1997) *BioEssays* **19,** 967–975.
15. Kelman, Z. (1997) *Oncogene* **14,** 629–640.
16. Kong, X.-P., Onrust, R., O'Donnel, M. & Kuriyan, J. (1992) *Cell* **69,** 425–437.
17. Kuriyan, J. & O'Donnel, M. (1993) *J. Mol. Biol.* **234,** 915–925.
18. Krishna, T. S., Kong, X. P., Gary, S., Burgers, P. M. J. & Kuriyan, J. (1994) *Cell* **79,** 1233–1243.
19. Gulbis, J. M., Kelman, Z., Hurwitz, J., O'Donnell, M. & Kuriyan, J. (1996) *Cell* **87,** 297–306.
20. Prelich, G., Tan, C.-K., Kostura, M., Mathews, M. B., So, A. G., Downey, K. M. & Stillman, B. (1987) *Nature (London)* **326,** 517–519.
21. Bravo, R., Frank, R., Blundell, P. A. & Macdonald-Bravo, H. (1987) *Nature (London)* **326,** 515–517.
22. Yao, N., Turner, J., Kelman, Z., Stukenberg, P. T., Dean, F., Shechter, D., Pan, Z. Q., Hurwitz, J. & O'Donnell, M. (1996) *Genes Cells* **1,** 101–113.
23. O'Donnell, M., Onrust, R., Dean, F. B., Chen, M. & Hurwitz, J. (1993) *Nucleic Acids Res.* **21,** 1–3.
24. Gerik, K. J., Gary, S. J. & Burgers, P. M. J. (1997) *J. Biol. Chem.* **272,** 1256–1262.
25. Tsurimoto, T. & Stillman, B. (1990) *Proc. Natl. Acad. Sci. USA* **87,** 1023–1027.
26. Yoder, B. L. & Burgers, P. M. J. (1991) *J. Biol. Chem.* **266,** 22689–22697.
27. Cai, J., Yao, N., Gibbs, E., Finkelstein, J., Phillips, B., O'Donnell, M. & Hurwitz, J. (1998) *Proc. Natl. Acad. Sci. USA* **95,** 11607–11612.
28. Hingorani, M. M. & O'Donnell, M. (1998) *J. Biol. Chem.* **273,** 24550–24563.
29. Turner, J., Hingorani, M. M., Kelman, Z. & O'Donnell, M. (1999) *EMBO J.* **18,** 771–783.
30. Fukuda, K., Morioka, H., Imajou, S., Ikeda, S., Ohtsuka, E. & Tsurimoto, T. (1995) *J. Biol. Chem.* **270,** 22527–22534.
31. Adachi, Y., Usukura, J. & Yanagida, M. (1997) *Genes Cells* **2,** 467–479.
32. Hirako, Y., Usukura, J., Nishizawa, Y. & Owaribe, K. (1996) *J. Biol. Chem.* **271,** 13739–13745.
33. Hirako, Y., Usukura, J., Uematsu, J., Hashimoto, T., Kitajima, Y. & Owaribe, K. (1998) *J. Biol. Chem.* **273,** 9711–9717.
34. Shao, Z., Yang, J. & Somlyo, A. P. (1995) *Annu. Rev. Cell. Dev. Biol.* **11,** 241–265.
35. Nishijima, H., Kamo, S., Akita, S., Nakayama, Y., Hohmura, K. I., Yoshimura, S. H. & Takeyasu, K. (1999) *Appl. Phys. Lett.* **74,** 4061–4063.
36. Waga, S. & Stillman, B. (1998) *Mol. Cell. Biol.* **7,** 4177–4187.
37. Zhang, G., Gibbs, E., Kelman, Z., O'Donnell, M. & Hurwitz, J. (1999) *Proc. Natl. Acad. Sci. USA* **96,** 1869–1874.
38. Natsume, T., Koide, T., Yokota, S., Hirayoshi, K. & Nagata, K. (1994) *J. Biol. Chem.* **269,** 31224–31228.
39. Yoder, B. L. & Burgers, P. M. (1991) *J. Biol. Chem.* **266,** 22689–22697.
40. Suzuki, Y., Yasunaga, T., Ohkura, R., Wakabayashi, T. & Sutoh, K. (1998) *Nature (London)* **396,** 380–383.
41. Baird, C. L., Harkins, T. T., Morris, S. K. & Lindsley, J. E. (1999) *Proc. Natl. Acad. Sci. USA* **96,** 13685–13690.
42. Hingorani, M. M., Bloom, L. B., Goodman, M. F. & O'Donnell, M. (1999) *EMBO J.* **18,** 5131–5144.
43. Tsurimoto, T. & Stillman, B. (1991) *J. Biol. Chem.* **266,** 1950–1960.
44. Zhang, G., Gibbs, E., Kelman, Z., O'Donnell, M. & Hurwitz, J. (1999) *Proc. Natl. Acad. Sci. USA* **96,** 1869–1874.
45. Tsurimoto, T. & Stillman, B. (1989) *EMBO J.* **8,** 3883–3889.
46. Podust, V., Mikhailov, V., Georgaki, A. & Hubscher, U. (1992) *Chromosoma* **102,** S133–S141.
47. Lee, S. H., Kwong, A. D., Pan, Z. Q. & Hurwitz, J. (1991) *J. Biol. Chem.* **266,** 594–602.
48. Mossi, R., Jonsson, Z. O., Allen, B. L., Hardin, S. H. & Hubscher, U. (1997) *J. Biol. Chem.* **272,** 1769–1776.
49. Bell, S. P. & Stillman, B. (1992) *Nature (London)* **357,** 128–134.
50. Kearsey, S. E. & Labib, K. (1998) *Biochim. Biophys. Acta* **1398,** 113–136.
51. Alberts, B. (1998) *Cell* **92,** 291–294.